PROCEEDINGS OF SCIENCE

Production of light nuclei in small collision systems measured with ALICE

Alessandro Balbino*, **on behalf of the ALICE Collaboration**

Politecnico di Torino,
24, Corso Duca degli Abruzzi, Turin, Italy
INFN di Torino,
1, Via Pietro Giuria, Turin, Italy

E-mail: alessandro.balbino@polito.it

The energy densities reached in high-energy hadronic collisions at the LHC allow significant production of light (anti)nuclei. Their production yields have been measured as a function of p_{T} and charged-particle multiplicity in the ALICE detector for different collision systems and at different center-of-mass energies. One of the most interesting results obtained from such a large variety of experimental data is that the dominant production mechanism of light (anti)nuclei seems to depend solely on the event charged-particle multiplicity. Evidence for this comes from the continuous evolution of the coalescence parameter, the deuteron-to-proton and the ^{3}He-to-proton ratios with the event multiplicity across different collision systems and energies. The characterization of the light nuclei production mechanism is complemented by measurements of their production yields in jets, where hard QCD processes are dominant, and in the underlying event, which is dominated by soft QCD processes. In this contribution, recent results on the measurements of light nuclei production in proton-proton and proton-lead collisions at different center-of-mass energies are shown and discussed in the context of the statistical hadronization and coalescence models.

**** The European Physical Society Conference on High Energy Physics (EPS-HEP2021), ****
**** 26-30 July 2021 ****
**** Online conference, jointly organized by Universität Hamburg and the research center DESY ****

*Speaker

PoS(EPS-HEP2021)392

1. Nuclear matter production

Although at the LHC light (anti)nuclei are abundantly produced, their production mechanisms are not completely understood. The light nuclei are characterised by a low binding energy ($E_{\rm B} \sim 1$ MeV) compared to the temperature of chemical freeze-out, which is the stage in the hadronization process when the abundance of particle species is fixed ($T_{\rm ch} \sim 160$ MeV). The study of light nuclei production and the comparison with the predictions of theoretical models are crucial to understand how these loosely bound objects can be formed and survive in such extreme conditions. Two classes of phenomenological models are available, namely the statistical hadronisation [1] and the coalescence [2] models. According to the statistical hadronisation model (SHM), (anti)nuclei are produced at the chemical freeze-out, along with all the other hadrons. The SHM can describe the production yields ($\frac{{\rm d}N}{{\rm d}y}$) in central Pb–Pb collisions [3], including yields of nuclei, using only three parameters: temperature T, volume V and baryo-chemical potential $\mu_{\rm B}$. In Pb–Pb collisions a grand canonical approach is used, since the condition $VT^3 > 1$ is satisfied, where V and T are the system volume and temperature, respectively. In pp and p–Pb collisions, characterised by a smaller volume, this condition is not met and hence a canonical approach is used. In the canonical statistical model (CSM) the local conservation of quantum numbers is required. In this work, the data are compared with the prediction of THERMAL-FIST package [4], in which baryon number, strangeness content and electric charge are exactly conserved. In the coalescence picture, nucleons that are close to each other in phase space after chemical freeze-out can form a nucleus via coalescence [2]. The main observable of the model is the coalescence parameter, defined for a nuclei of mass number A as:

$$B_{\rm A} = \frac{E_i \frac{{\rm d}^3 N_{\rm i}}{{\rm d}p_{\rm i}^3}}{\left(E_{\rm p} \frac{{\rm d}^3 N_{\rm p}}{{\rm d}p_{\rm p}^3}\right)^A} \tag{1}$$

where the invariant spectra of the (anti)protons are evaluated at the transverse momentum of the nucleus divided by its mass number, so that $p_{\rm T}^{\rm p} = p_{\rm T}^{\rm A}/A$. The coalescence parameter is related to the probability to form a nucleus via coalescence [2]. Moreover, studies of the Underlying Event (UE) can provide valuable insight when investigating nuclei production in small systems. The UE is defined as the collection of all particles not originating from the primary scattering and it is analysed by measuring particle production in three azimuthal regions: toward, transverse and away, with respect to the highest-momentum track of a given event. In the transverse region the particle density eventually becomes mostly insensitive to the hard component and the particle production is driven by soft QCD processes, while hard interactions are dominant in the toward and away regions. In this context the activity in the UE can be quantified using the self-normalised charged-particle multiplicity in the transverse region $R_{\rm T} = \frac{N_{\rm ch,T}}{\langle N_{\rm ch,T} \rangle}$. Small values of $R_{\rm T}$ correspond to an event topology dominated by the hard scattering, while large $R_{\rm T}$ values correspond to events characterized by large UE activity.

2. The coalescence parameter

The coalescence parameter $B_{\rm A}$ has been measured in different collision systems as a function of the transverse momentum ($p_{\rm T}$). In Fig. 1, B_2 in pp collisions at $\sqrt{s} = 13$ TeV and B_3 in p–Pb

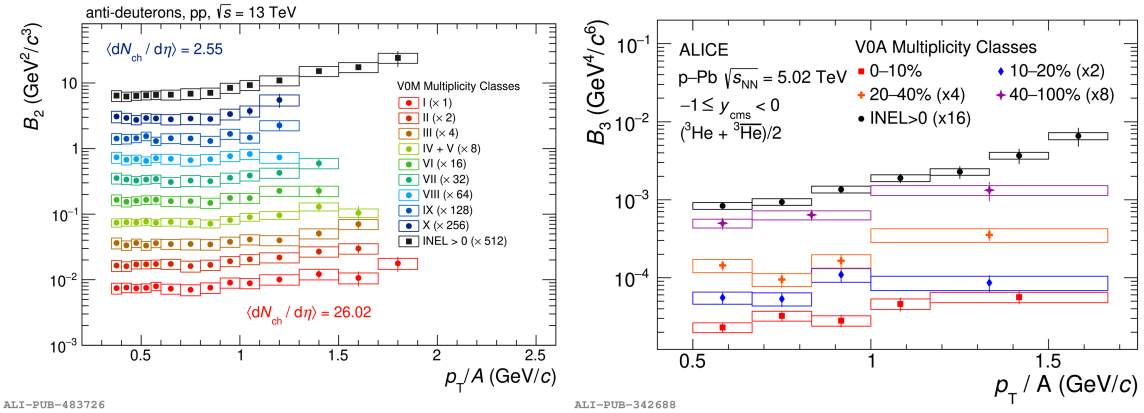

Figure 1: B_2 as a function of p_{T}/A in pp collisions at $\sqrt{s}$ = 13 TeV (left) and B_3 in p–Pb collisions at $\sqrt{s_{\mathrm{NN}}}$ = 5.02 TeV (right) for different multiplicity intervals.

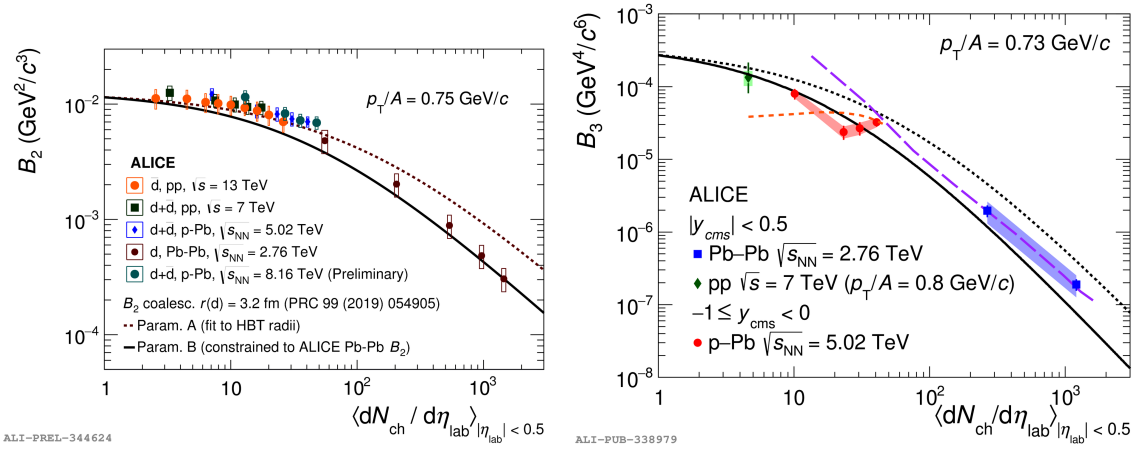

Figure 2: B_2 [5–8] (left) and B_3 [5, 9, 10] (right) as a function of the average event multiplicity $\langle \frac{\mathrm{d}N_{\mathrm{ch}}}{\mathrm{d}\eta} \rangle$ at $p_{\mathrm{T}}/A = 0.75$ GeV/c and at $p_{\mathrm{T}}/A = 0.73$ GeV/c, respectively. Data are compared with the predictions of the coalescence model. The dashed line and the black continuous one correspond to different parameterisations of $\langle \frac{\mathrm{d}N_{\mathrm{ch}}}{\mathrm{d}\eta} \rangle$ with respect to the HBT radius.

collisions at $\sqrt{s_{\mathrm{NN}}} = 5.02$ TeV for different multiplicity intervals are shown.

In pp collisions, B_2 shows a minor increase over the p_{T} range. In p–Pb collisions, a considerable increase of B_3 with increasing p_{T} is observed. The dependence of the B_{A} on the system size can be studied by measuring for each collision system and energy the value of B_{A} as a function of charged particle multiplicity $\langle \frac{\mathrm{d}N_{\mathrm{ch}}}{\mathrm{d}\eta} \rangle$, which is related to the system size. Figure 2 shows B_2 and B_3 as a function of $\langle \frac{\mathrm{d}N_{\mathrm{ch}}}{\mathrm{d}\eta} \rangle$ at $p_{\mathrm{T}}/A = 0.75$ GeV/c and at $p_{\mathrm{T}}/A = 0.73$ GeV/c, respectively.

Data are compared with the calculations for the coalescence model for two different parameterisations of the system size. B_{A} evolves smoothly as a function of $\langle \frac{\mathrm{d}N_{\mathrm{ch}}}{\mathrm{d}\eta} \rangle$, regardless of the collision system, suggesting a common production mechanism that depends only on the system size. At low multiplicity the system size is smaller than the nucleus size and B_{A} slightly decreases with multiplicity. On the other hand, at high multiplicity the system size becomes larger than the size of

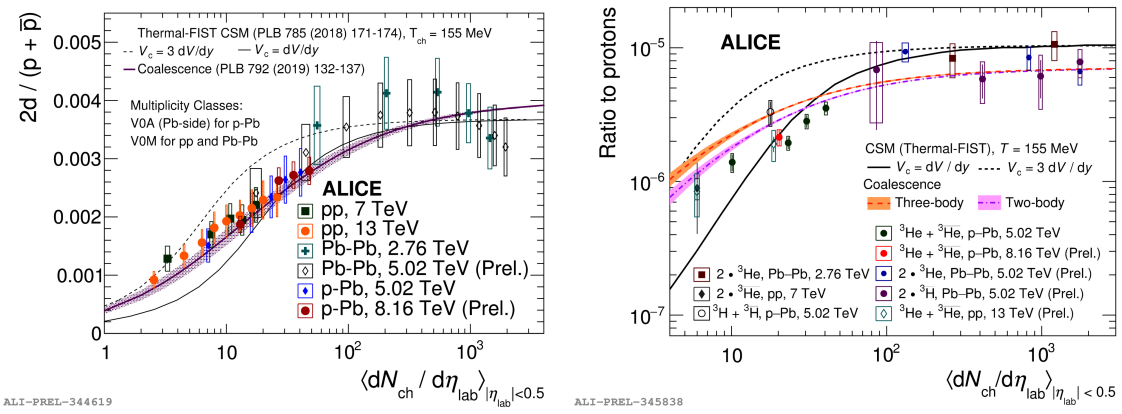

Figure 3: Ratio between the p_{T}-integrated yields of nuclei and protons for deuterons (d/p) [5–8] (left), ^{3}He (^{3}He/p [5, 9, 10]) and ^{3}H (^{3}H/p [10]) (right). Data are compared with the predictions of the THERMAL-FIST package [4] and the coalescence model [11].

the nucleus and hence the decrease is more noticeable. Therefore, the global trend observed in the data is described by the coalescence model.

3. The ratio between nucleus and proton yields

In Fig. 3 the ratio between the p_{T}-integrated yields of nuclei and protons are shown for deuterons (d/p), ^{3}He (^{3}He/p) and ^{3}H (^{3}H/p).

Data are compared with the prediction of SHM obtained with the THERMAL-FIST package and with coalescence calculations [11]. For ^{3}He, results from both the two-body and the three-body coalescence are reported. The yield ratios evolve smoothly as a function of multiplicity, as observed for B_{A}. This is another hint of a common particle production mechanism that depends only on the system size. In both the panels of Fig. 3, two regimes can be seen. In the low multiplicity region, the yield ratios increase with multiplicity. The agreement of multiplicity dependence of yield ratios with CSM arises because of canonical suppression which is a consequence of conservation of baryon number [4]. The area between the solid and dashed lines represents the prediction of CSM for values of the source volume from 1 to 3 rapidity units and a temperature T = 155 MeV. Experimental data suggest a source volume between 1 and 3 units of rapidity. In the coalescent picture, the rise at low multiplicity reflects the interplay between nucleon yield, nucleus size and source size. Both CSM and coalescence models can qualitatively describe the ratio between the yields of nuclei and protons, except for nuclei with $A \geq 3$ in the intermediate multiplicity region. In the high multiplicity region, the conditions for description using the grand canonical model are valid. The experimental results show no dependence on multiplicity as predicted by the models. The coalescence models also predict a saturation of the yield ratio at high multiplicity.

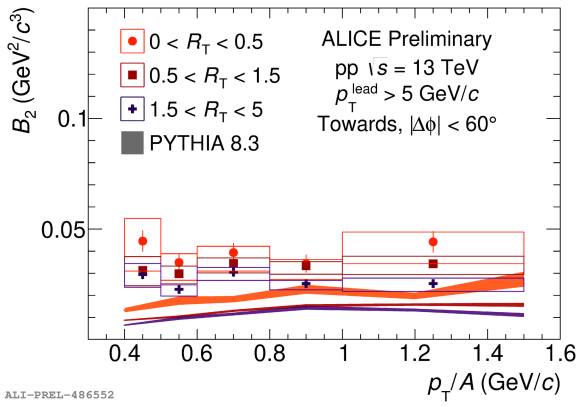

Figure 4: B_2 as a function of p_T/A in pp collisions at $\sqrt{s}$ = 13 TeV in the toward region, for several R_T classes. Data are compared with the predictions from Pythia 8.3.

4. Underlying Event activity

In Fig. 4, B_2 measured in pp collisions at $\sqrt{s}$ = 13 TeV in the toward region, for several R_T classes, is compared with the expectations of Pythia 8.3 [12] simulations. The B_2 parameter has a flat behaviour with p_T/A for all the R_T regions and is in agreement with the predictions of a simple coalescence picture. Pythia 8.3 simulations can qualitatively reproduce the p_T dependence and the mild R_T ordering. However, Pythia fails in reproducing the magnitude of the coalescence parameter. Moreover it was observed that deuterons are mostly produced in the underlying event: the recent results of deuteron production in jets [13] have shown that the fraction of deuterons produced in the jet is between 8 and 15 %, increasing with increasing p_T, while the majority of the deuterons are produced in the underlying event.

5. Conclusions

The measurements of the coalescence parameter B_A and of the yield ratios d/p, ^{3}He/p and ^{3}H/p as a function of the event multiplicity suggest a common production mechanism that depends only on the system size. Coalescence can describe both the B_A and the yield ratios as a function of multiplicity. CSM can qualitatively describe the evolution of yield ratios with the system size. Using the current experimental results, it is not possible to discern between the different production mechanisms of light nuclei. Moreover, the study of the deuterons produced in the underlying event showed that the deuteron production is dominated by soft QCD processes, but larger data samples would be needed in order to obtain more precise results and to expand this kind of analysis to other nuclear species. However, the current ALICE upgrade campaign will allow data acquisition during LHC Run 3 with a new Inner Tracking System, whose high granularity, improved geometry and very low material budget will facilitate the measurement of (anti)nuclei in ALICE, leading to smaller systematic uncertainties. Moreover with the increased data-acquisition rate it will be possible to search for the production of heavier nuclei in small systems. With these improvements, it may be possible to better understand the phenomena underlying the production of light nuclei.

References

[1] A. Andronic, P. Braun-Munzinger, J. Stachel and H. Stocker, *Production of light nuclei, hypernuclei and their antiparticles in relativistic nuclear collisions*, *Phys. Lett. B* **697** (2011) 203 [1010.2995].

[2] J.I. Kapusta, *Mechanisms for deuteron production in relativistic nuclear collisions*, *Phys. Rev. C* **21** (1980) 1301.

[3] ALICE collaboration, *Production of ^{4}He and $^4\overline{\text{He}}$ in Pb-Pb collisions at $\sqrt{s_{\text{NN}}} = 2.76$ TeV at the LHC*, *Nucl. Phys. A* **971** (2018) 1 [1710.07531].

[4] V. Vovchenko, B. Dönigus and H. Stoecker, *Multiplicity dependence of light nuclei production at LHC energies in the canonical statistical model*, *Phys. Lett. B* **785** (2018) 171 [1808.05245].

[5] ALICE collaboration, *Production of light nuclei and anti-nuclei in pp and Pb-Pb collisions at energies available at the CERN Large Hadron Collider*, *Phys. Rev. C* **93** (2016) 024917 [1506.08951].

[6] ALICE collaboration, *(Anti-)deuteron production in pp collisions at $\sqrt{s}$ = 13 TeV*, *Eur. Phys. J. C* **80** (2020) 889 [2003.03184].

[7] ALICE collaboration, *Multiplicity dependence of (anti-)deuteron production in pp collisions at $\sqrt{s} = 7$ TeV*, *Phys. Lett. B* **794** (2019) 50 [1902.09290].

[8] ALICE collaboration, *Multiplicity dependence of light (anti-)nuclei production in p-Pb collisions at $\sqrt{s_{\text{NN}}} = 5.02$ TeV*, *Phys. Lett. B* **800** (2020) 135043 [1906.03136].

[9] ALICE collaboration, *Production of deuterons, tritons, ^{3}He nuclei and their antinuclei in pp collisions at $\sqrt{s} = 0.9$, 2.76 and 7 TeV*, *Phys. Rev. C* **97** (2018) 024615 [1709.08522].

[10] ALICE collaboration, *Production of (anti-)^{3}He and (anti-)^{3}H in p-Pb collisions at $\sqrt{s_{\text{NN}}} = 5.02$ TeV*, *Phys. Rev. C* **101** (2020) 044906 [1910.14401].

[11] F. Bellini and A.P. Kalweit, *Testing production scenarios for (anti-)(hyper-)nuclei and exotica at energies available at the CERN Large Hadron Collider*, *Phys. Rev. C* **99** (2019) 054905 [1807.05894].

[12] T. Sjöstrand, *The PYTHIA Event Generator: Past, Present and Future*, *Comput. Phys. Commun.* **246** (2020) 106910 [1907.09874].

[13] ALICE collaboration, *Jet-associated deuteron production in pp collisions at s=13 TeV*, *Phys. Lett. B* **819** (2021) 136440 [2011.05898].

PoS(EPS-HEP2021)392